



# EUROfusion

EUROFUSION WPJET2-CP(16) 15119

AM Widdowson et al.

## **Overview of fuel inventory in JET with the ITER-Like Wall**

Preprint of Paper to be submitted for publication in  
Proceedings of 26th IAEA Fusion Energy Conference



This work has been carried out within the framework of the EUROfusion Consortium and has received funding from the Euratom research and training programme 2014-2018 under grant agreement No 633053. The views and opinions expressed herein do not necessarily reflect those of the European Commission.

This document is intended for publication in the open literature. It is made available on the clear understanding that it may not be further circulated and extracts or references may not be published prior to publication of the original when applicable, or without the consent of the Publications Officer, EUROfusion Programme Management Unit, Culham Science Centre, Abingdon, Oxon, OX14 3DB, UK or e-mail [Publications.Officer@euro-fusion.org](mailto:Publications.Officer@euro-fusion.org)

Enquiries about Copyright and reproduction should be addressed to the Publications Officer, EUROfusion Programme Management Unit, Culham Science Centre, Abingdon, Oxon, OX14 3DB, UK or e-mail [Publications.Officer@euro-fusion.org](mailto:Publications.Officer@euro-fusion.org)

The contents of this preprint and all other EUROfusion Preprints, Reports and Conference Papers are available to view online free at <http://www.euro-fusionscipub.org>. This site has full search facilities and e-mail alert options. In the JET specific papers the diagrams contained within the PDFs on this site are hyperlinked

## Overview of Fuel Inventory in JET with the ITER-Like Wall

A. Widdowson<sup>1</sup>, E. Alves<sup>2</sup>, A. Baron-Wiechec<sup>1</sup>, N.P. Barradas<sup>3</sup>, J. Beal<sup>1</sup>, N. Catarino<sup>2</sup>, J.P. Coad<sup>1</sup>, V. Corregidor<sup>2</sup>, K. Heinola<sup>4</sup>, S. Koivuranta<sup>5</sup>, S. Krat<sup>6,7</sup>, A. Lahtinen<sup>4</sup>, J. Likonen<sup>5</sup>, G.F. Matthews<sup>1</sup>, M. Mayer<sup>6</sup>, P. Petersson<sup>8</sup> and M. Rubel<sup>8</sup> and JET Contributors\*

EUROfusion Consortium, JET, Culham Science Centre, Abingdon, OX14 3DB, UK

<sup>1</sup>Culham Centre for Fusion Energy, Culham Science Centre, Abingdon, OX14 3DB, UK

<sup>2</sup>IPFN Instituto Superior Técnico, Universidade de Lisboa, 1049-001 Lisboa, Portugal

<sup>3</sup>C2TN, Instituto Superior Técnico, Universidade de Lisboa, 2695-066 Lisboa, Portugal

<sup>4</sup>University of Helsinki, P.O. Box 64, 00560 Helsinki, Finland

<sup>5</sup>VTT Technical Research Centre of Finland, P.O. Box 1000, FIN-02044 VTT, Finland

<sup>6</sup>Max-Planck Institut für Plasmaphysik, 85748 Garching, Germany

<sup>7</sup>National Research Nuclear University MEPhI, 115409 Moscow, Russia

<sup>8</sup>Royal Institute of Technology, SE-10044 Stockholm, Sweden

\* See the author list of “Overview of the JET results in support to ITER” by X. Litaudon et al. to be published in Nuclear Fusion Special issue: overview and summary reports from the 26th Fusion Energy Conference (Kyoto, Japan, 17-22 October 2016)

*E-mail contact of main author: [anna.widdowson@ukaea.uk](mailto:anna.widdowson@ukaea.uk)*

**Abstract.** Post mortem analyses of JET ITER-Like-Wall tiles and passive diagnostics have been completed after each of the first two campaigns (ILW-1 and ILW-2). They show that the global fuel inventory is still dominated by deposition; hence plasma parameters and sputtering processes affecting material migration influence the distribution of retained fuel. In particular, differences between results from the two campaigns may be attributed to a greater proportion of pulses run with strike points in the divertor corners, and having about 300 discharges in hydrogen at the end of ILW-2. Recessed and remote areas can contribute to fuel retention due to the larger areas involved, e.g. recessed main chamber walls, gaps in castellated Be main chamber tiles and material migration to remote divertor areas. The fuel retention and material migration due to the bulk W Tile 5 during ILW-1 are presented. Overall these tiles account for only a small percentage of the global accountancy for ILW-1.

### 1. Introduction

JET is the largest operating tokamak in the world, and holds the records for fusion power parameters such as attained Q values and neutron production [1]. Since 1989 JET has used beryllium (Be) as a first wall component, and first used tritium (T) fuelling in 1991 [2]. Because of the potential hazard to health from these materials, JET has developed sophisticated remote handling techniques for use in the vessel to minimize exposure to operatives. In 2010-11 all the plasma-facing components within JET (which were mostly carbon) were stripped out and replaced with predominantly Be in the main chamber and tungsten in the divertor, which is the material mix that will be used for ITER: the new configuration is termed the “JET ITER-like Wall” (JET-ILW) [3]. In the main chamber the plasma-interacting components (limiters) are of solid Be, whilst other plasma-facing surfaces

are coated with Be. In the divertor all tiles are carbon-fibre composite with plasma facing surfaces coated with tungsten (W) except for one ring of tiles which are of solid W. There have been two completed operational campaigns with JET-ILW; the first in 2011-12 (ILW-1) and second in 2013-14 (ILW-2) [4]. The gas balance measurements that were made are of particular relevance to this paper, and have shown that following ILW-1 the amount of fuel retained (normally deuterium, D, in JET) was at least an order of magnitude lower than with the carbon wall configuration [4][5]. First wall components have been removed from JET during the shutdown after every operational campaign since the first in 1983. Following the

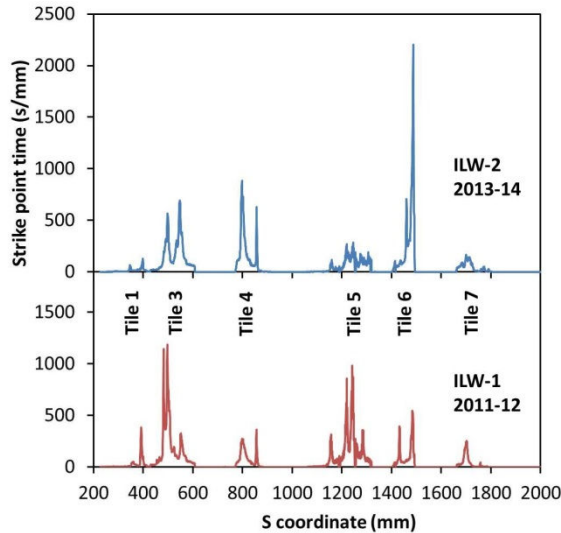


FIG. 1 Strike point distributions for ILW-1 and ILW2 campaigns.

restricting the first few plasmas to what is normally the start-up phase of a pulse when plasma current is increased within a circular cross-section in the main chamber which contacts only the limiters (referred to as “limiter phase”). For the remaining operating period strike points were formed at the inner and outer divertor surfaces (target plates) after the limiter start-up phase (referred to as “divertor phase”). Overall plasma times for ILW-1 and ILW-2 were similar:  $\sim 6/5$  hours limiter phase plasma and  $\sim 13/14$  hours divertor phase plasma, counting only discharges with plasma current  $>0.25$  MA. JET operational campaigns invariably explore a range of plasma parameters such as shape, additional heating scenarios, etc., however ILW-1 concentrated on plasma parameters most relevant to ITER; specifically, the influence of the inner and outer strike point (ISP and OSP, respectively) locations on global material migration and fuel retention. The comparison between strike point distributions for ILW-1 and ILW-2 is shown in FIG. 1 and the ramifications will be elaborated in the next section.

Throughout ILW-1 the predominant fuelling gas was D, and the last 125 discharges were with the same plasma configuration, whereas ILW-2 ended

the introduction of Be and T the removal of components has been undertaken by remote handling. Post mortem analysis of these components provides an overall picture of material migration and long term fuel inventory. This has been particularly important for the JET-ILW to study the differences from the behaviour with a carbon first wall and the likely benefits for ITER. Results from ILW-1 and ILW-2 JET-ILW campaigns are now available making a comprehensive overview possible.

## 2. Experimental Details

The first experiments of ILW-1 were an assessment of the resilience of the Be limiters in the main chamber. This was achieved by restricting the first few plasmas to what is normally the start-up phase of a pulse when plasma current is increased within a circular cross-section in the main chamber which contacts only the limiters (referred to as “limiter phase”). For the remaining operating period strike points were formed at the inner and outer divertor surfaces (target plates) after the limiter start-up phase (referred to as “divertor phase”). Overall plasma times for ILW-1 and ILW-2 were similar:  $\sim 6/5$  hours limiter phase plasma and  $\sim 13/14$  hours divertor phase plasma, counting only discharges with plasma current  $>0.25$  MA. JET operational campaigns invariably explore a range of plasma parameters such as shape, additional heating scenarios, etc., however ILW-1 concentrated on plasma parameters most relevant to ITER; specifically, the influence of the inner and outer strike point (ISP and OSP, respectively) locations on global material migration and fuel retention. The comparison between strike point distributions for ILW-1 and ILW-2 is shown in FIG. 1 and the ramifications will be elaborated in the next section.

TABLE I Fuel inventory for different JET-ILW divertor and main chamber surfaces following ILW-1.

Shading = remote/recessed surface.

\* ref [6], † new data, ‡ ref [18].

Divertor Tungsten	Inventory ( $10^{22}$ D atoms)	Main chamber Beryllium	Inventory ( $10^{22}$ D atoms)
Inner divertor*	17	Inner limiters*	1.4
Outer divertor*	3.9	Outer limiters*	5.2
Bulk tungsten†	0.3	Dump plate*	2.1
Inner corner*	2.0	Inner wall*	2.8
Outer corner*	2.2	Outer wall*	0.9
		Castellation gaps‡	1.0

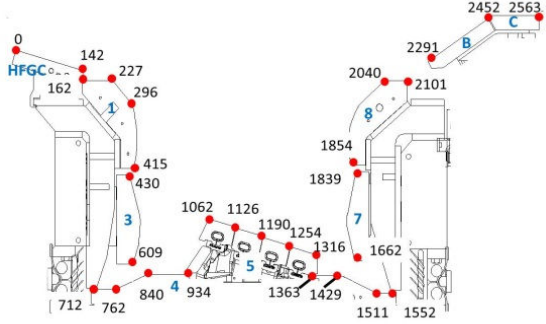


FIG. 2 Cross section of JET-ILW divertor showing tile numbering and the  $s$ -coordinate; distance around the divertor surface in millimetres.

following ILW-1 is shown in TABLE I. The global long term fuel retention in ILW-1 was  $\sim 0.2\%$  of injected fuel - at least an order of magnitude lower than with the carbon wall configuration, in agreement with the gas balance measurements referred to in section 1. Of this  $\sim 65\%$  of the retained D was found in the divertor, with the remaining inventory located in the main chamber [6]. Fuel retention in JET is still dominated by co-deposition at the inner divertor,  $17 \times 10^{22}$  D atoms, however now the thick deposits are at the inner top horizontal surfaces of Tile 1 and the HFGC tile, reaching  $15 \mu\text{m}$  after ILW-1 and increasing to  $>20 \mu\text{m}$  after ILW-2. This contrasts to all the campaigns with a carbon wall and divertor wherein the majority of the deposits collected at the inner corner of the divertor [7]. Overall the outer divertor surfaces remained a net erosion zone and had a lower fuel inventory,  $3.9 \times 10^{22}$  D atoms. Fuel retained on the bulk tungsten load-bearing plate at the base of the divertor was  $\sim 3 \times 10^{21}$  D atoms following ILW-1. This contributes only a small inventory to the divertor and is consistent with the surface being a net erosion zone.

Deposition in the inner divertor following ILW-2 extends further down the vertical surfaces of Tile 1 (see FIG. 2) as shown in FIG. 3, and this is because there were many more ISP in the inner corner on Tile 4 when this part of Tile 1 was deeper into the inner scrape-off layer (SOL) than for ILW-1, and this is the region where deposition of impurities dominates over erosion by energetic D ions. The deposits on Tile 1 were thicker after ILW-2, so that although the concentration of retained D within the deposits was similar for the two campaigns as has been shown using SIMS, the overall amount retained was greater for ILW-2, as shown in FIG. 3 SIMS also showed that there were elevated concentrations of H at the surface following ILW-2, see FIG. 4, and this must be due to the fact that for the last 300 discharges of ILW-2

with a hydrogen (H) campaign with a programme of varied plasma configurations. Approximately 300 ILW-2 pulses were performed in H,  $\sim 10\%$  of the total number of JET pulses throughout the campaign.

### 3. Results

#### 3.1 Divertor Retention

A cross-section of the JET divertor is shown in FIG. 2 which gives the tile numbers and the distances (in millimetres) around the divertor (“ $s$ -coordinates”). The distribution of retained D fuel on the inner and outer divertor surfaces

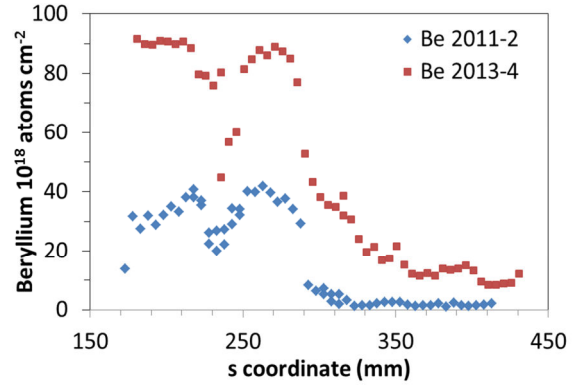


FIG. 3 Distribution of Be along Tile 1 for ILW-1 and ILW-2

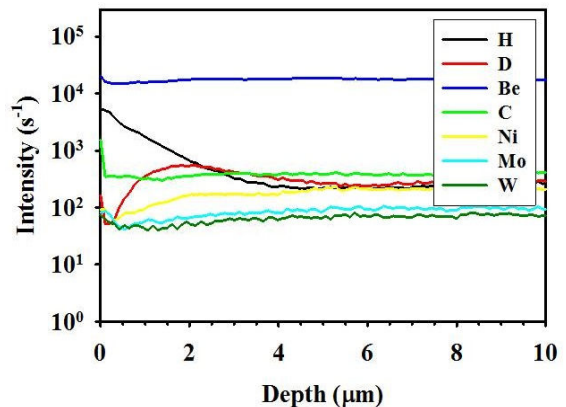


FIG. 4 SIMS data showing increased H (black) at the surface

the plasma was fuelled by H instead of D resulting in isotope exchange at the surface; the ILW-1 campaign finished directly with D fuelling. Further evidence for this effect can be seen in the Ion Beam Analysis (IBA) variant Nuclear Reaction Analysis (NRA), which indicated

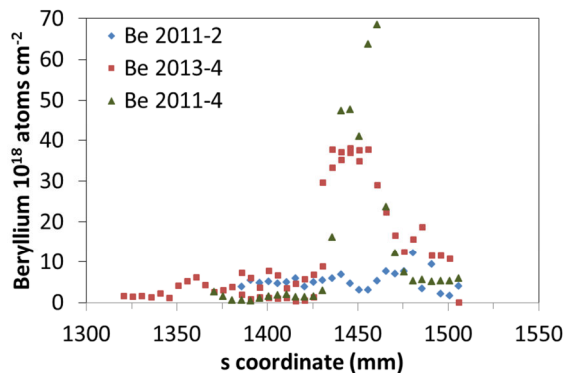


FIG. 5 Be concentration across Tile 6 after various periods of exposure

that D was of approximately uniform concentration in the outermost few microns after ILW-2 whereas there was additionally a strong surface D peak after ILW-1.

The surfaces of the outer divertor Tiles 7 and 8 show negligible concentrations of Be and other plasma impurities and have a low fuel inventory consistent with D implantation only, indicating they are net erosion zones when compared with the inner divertor which is a net deposition zone. As the tile surfaces are W-coated it requires energetic ions to cause any measurable erosion, but nevertheless

erosion of coatings on the horizontal top surface of Tile 8 is evident from microscopy studies of cross sections. The only region of significant deposit on outer divertor tiles is on Tile 6, where a band of beryllium (Be) deposit has formed at the bottom of the sloping part of the tile, which is just beyond the strike point accessible region in the entrance to the pump duct. Although visible after ILW-1, the deposit was much thicker after ILW-2 (Be  $\sim 3.8 \times 10^{19}$  atoms  $\text{cm}^{-2}$ , FIG. 5), and is layered as shown in FIG. 6. The balance between erosion and deposition in the outer corner is very much dependent on plasma conditions during campaigns; for example the band of Be deposition is  $\sim 5$  times higher for ILW-2 compared with ILW-1. This was likely due to the outer SP being located on the outer corner tile approximately 4 times longer during ILW-2 than ILW-1 (see FIG. 1); therefore more material is transported to this region. Plasma exposed regions show  $< 10^{18}$  D atoms  $\text{cm}^{-2}$  whereas shadowed regions are up to a factor of 10 times higher where there is some co-deposition with Be. However, these D concentrations also indicate that they are limited by strong plasma interaction resulting in raised surface temperatures. There are many devices for measuring deposition and retention in the corner regions such as louvre clips, deposition monitors, etc. [8], and from IBA measurements on these devices the contributions of the shadowed areas to the D inventory after ILW-1 were estimated (see TABLE I).

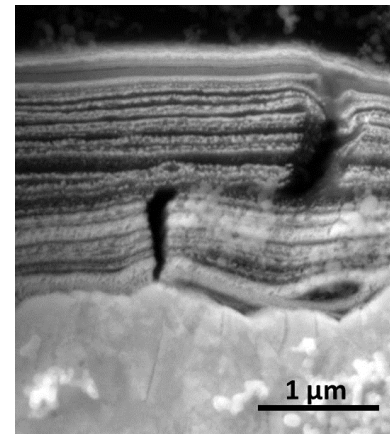


FIG. 6 Layered structure of deposit on Tile 6 from ILW-1

Lower accumulated deposits in JET-ILW have a direct impact on the amount of dust and flakes forming in the vessel. However, it is also clear that the structure of Be deposits is much less friable than those of C: spalling of C deposits was frequently observed for films thinner than the Be-based deposits observed on Tile 1, and C deposits were dusty when rubbed, whereas Be deposits adhere well in tests with adhesive pads. The amount of dust collected via vacuuming of the divertor surfaces is  $\sim 1$  g/campaign, with currently no evidence of large scale spalling from deposits after ILW-2. This compares with  $\sim 200$  g for vacuuming of comparable surfaces of the JET-C divertor [9]. Analysis of the relatively few particles from JET-ILW indicate a range of sources including agglomerates originating from coatings, melted droplets, and Be-rich flakes from deposits [10][11].



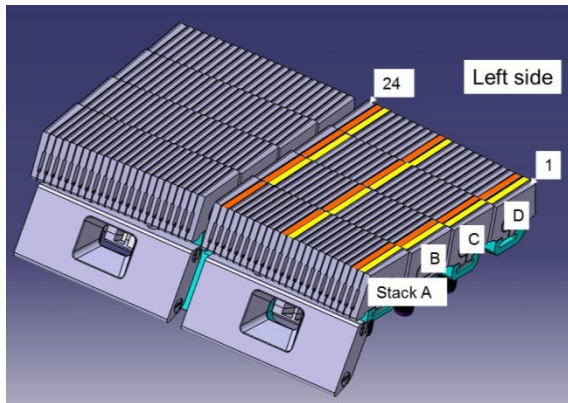


FIG. 7 Schematic of bulk W Tile 5. Lamellae analysed indicated in orange and yellow.

and the Be and C concentrations are generally  $<100\text{-}200 \times 10^{15}$  atoms  $\text{cm}^{-2}$ . The results show a complex distribution of D and Be concentrations due to the complex shape, however D concentrations are relatively higher in shadowed areas and lower in regions of higher surface temperature where the strike point was frequently located ( $s = 1242$  mm, see FIG. 1). The total plasma-facing surface area of the lamellae is  $3.312 \text{ m}^2$ : Allowing for some shadowing due to the “roof-top” effect, taking an average D concentration leads to an upper D fuel inventory of  $1.7 \times 10^{21}$  atoms. An evaluation of the D concentration in the gaps between lamellae shows the highest concentration of  $<10^{17}$  atoms  $\text{cm}^{-2}$  extending only a millimetre from the surface and falling to  $10^{15}$  atoms  $\text{cm}^{-2}$  at 10 mm. Assuming that most fuel is concentrated in the first millimetre from the top surface, the area in gaps contributing to fuel retention is  $1.1 \times 10^4 \text{ cm}^2$  giving an additional inventory from the gaps of  $1.1 \times 10^{21}$  atoms and bringing the total additional D inventory to  $2.8 \times 10^{21}$  atoms. This is  $\sim 1\%$  of the currently assessed inventory of  $20.9 \times 10^{22}$  atoms on divertor tiles (see TABLE I). By a similar analysis the number of Be atoms is  $6.3 \times 10^{23}$ , equivalent to  $\sim 0.1$  g Be, which is  $\sim 2\%$  of the currently assessed mass of deposits found in the divertor of 41-51 g for ILW-1 [12][13]. The maximum W erosion is observed at the strike point and is evaluated from IBA analysis of W/Mo marker coating as  $< 3 \mu\text{m}$  [14].

## 4. Main Chamber

### 4.1 Retention in Be limiters

Any contact of the plasma with its surroundings in the main chamber is designed to be with solid beryllium limiters; at the outer wall with Outer Poloidal Limiters (OPL), at the inner wall with Inner Wall Guard Limiters (IWGL), and at the top with Dump Plates (DP). These are castellated blocks of Be mounted on Inconel backing plates: “castellated” means there are poloidal and toroidal cuts  $\sim 15$  mm deep into the Be approximately every 12 mm in each direction, which allow for differential thermal expansion of the surface due to plasma interaction and increases surface resistivity – this structure is the same as will be used for the main chamber walls of ITER, though in ITER

### 3.2 Bulk Tungsten Plasma Facing Components in the Divertor

The analysis of the first bulk W plasma facing components from the divertor Tile 5 exposed during ILW-1, shown in FIG. 7, has now been completed and the results are extrapolated to provide fuel inventory values for the bulk W Tile 5. These values have so far been omitted from publications [6][12][13] as they were not available until this time. From IBA the bulk W Tile 5 is shown to be a net tungsten erosion area with only a small amount of D, Be and C: the D concentrations are generally  $<10^{17}$  atoms  $\text{cm}^{-2}$

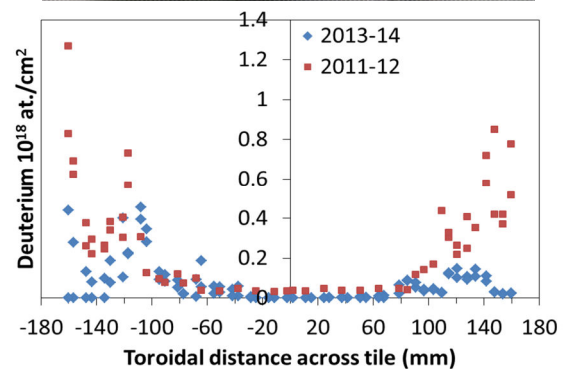
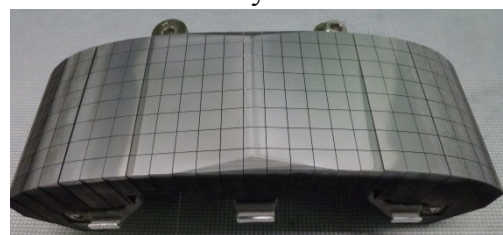


FIG. 8 Top: Photograph of an IWGL tile.  
Bottom: Comparison of the D concentrations across IWGL tile 2XR10 for tiles exposed during ILW-1 and ILW-2

the Be blocks will be bonded to water-cooled pipes. A photograph of an IWGL tile is included in FIG. 8. During plasma start-up the plasma is in contact with the main chamber limiters (mainly the IWGL), before switching to the X-point mode for the majority of the discharge when the main contact points are in the divertor. During the X-point phase contact with limiters is restricted to cross-field diffusion of ions through the scrape-off layer (SOL) plus bombardment by charge-exchange neutrals (CXN). For ILW-1 the total fuel inventory of plasma-facing main chamber tiles contributed  $\sim 30\%$  to the vessel inventory,  $8.7 \times 10^{22}$  D atoms see TABLE I.

During the limiter phases of the discharges, there is considerable erosion and re-deposition on the limiters. Analysis of individual inner limiter tiles show that the areas of highest erosion are at the centre of tiles near the mid-plane of JET, which are the points of plasma contact, and here fuel retention is very low. The toroidal distribution across limiter tiles shows higher concentrations of D at the ends of the tiles which is generally associated with re-deposition, as was described in [12]. There is also retention at all main chamber surfaces due to implantation by CXN and some co-deposition due to continued plasma interaction. There was a similar pattern of erosion and deposition on the IWGL resulting from ILW-2; FIG. 8 compares the D retention on a mid-plane IWGL tile in position 2XR10 which was exposed during ILW-1 with one exposed in the same location during ILW-2. Although the patterns are similar, the amount of D retained is significantly less following ILW-2, which may be the result of isotope exchange with H during the last 300 discharges of the campaign (as discussed in section 3.1); since the deposition/implantation layers are thin most of the retained hydrogen would be accessible for exchange. Reduced levels of D retention are also evident at the Be limiter exposed at the outer JET mid-plane during ILW-2 compared with one exposed in ILW-1. This could be due to either H exposure or alternatively that there may have been more plasma interaction (erosion) at this location during ILW-2.

Only limited areas of melting were seen on IWGL tiles resulting from either of the ILW campaigns [15], and none at all on OPL tiles, “extensive melting” at the Dump Plate tiles was reported after ILW-1 [16]. The melting was present on each row of DP tiles for a radial (poloidal) distance of about 1 metre, extending for a toroidal width of about one castellation immediately to one side of the ridge. However, there was much more widespread melting at the DP in evidence after ILW-2, even allowing for the fact that most of the tiles had now been exposed to the two campaigns rather than one. The melting extended radially outwards for an extra metre, and in width enveloped 2-3 castellations centred at the ridge. Part of this damage may occur during disruptions, which in JET have a predilection for travelling upwards to the top of the vessel. However, the incidence of disruptions during ILW-2 was comparable to ILW-1, and the increased radial extent is striking. Calculations of predicted power loads in ITER do indicate peaks in the top, outboard corner of ITER, and this appears to be manifested in JET. It is probable that melting in the DP region may be responsible for the examples of Be splashes and droplets of Be found in the JET divertor.

#### 4.2 Retention in Recessed Areas and Within Castellation Gaps

There are large areas of the main chamber wall that are not covered by limiters. During operations with the carbon wall the areas of the inboard (high-field) vessel wall within 1 metre above and below the mid-plane were covered with carbon tiles, and approximately half of the carbon impurity flux to the divertor was estimated to come from these areas as a result of CXN bombardment [17]. These areas are typically about 80 mm behind the leading edge of the IWGL. As this bombardment is the cause of much of the main chamber erosion, this area was covered with Inconel tiles coated with a layer of Be, (Inner Wall Cladding, IWC, tiles) to



ensure that Be is the predominant plasma impurity. It was not considered necessary to protect the outer vessel wall in the same way, since the outer wall is recessed by a much greater distance behind the OPL, and much of the area is covered by additional heating antennae or taken up by diagnostic and neutral beam access ports. An assessment of the amount of erosion at the IWC following ILW-1 indicated that the impurity flux of Be was about a factor of five less than the flux of C during the C-wall phase [13]. Since the overall reduction of deposition in the divertor with the JET ILW is of similar order, it follows that the IWC represent a similarly important source for the divertor deposition. The inner wall contributes  $2.8 \times 10^{22}$  atoms of D, or about 25%, to the retained main chamber inventory, whilst the contribution of the remainder of the main chamber wall is estimated at  $\frac{1}{4}$  of this value, as shown in TABLE I.

Each cut in the Be tiles made to form the castellations is about 0.4 mm wide, which is wide enough for a small amount of material to be deposited in the cut (gap). The deposition only extends for about 1 mm into the gap with typical D concentrations of  $\sim 6 \times 10^{17}$  atoms  $\text{cm}^{-2}$  for OPL and  $7\text{-}20 \times 10^{17}$  atoms  $\text{cm}^{-2}$  for IWGL, but  $<10^{17}$  atoms  $\text{cm}^{-2}$  for DP tiles. However, the total length of surfaces within castellations is  $\sim 7.3$  km, and the evaluation of D retained in the gaps between castellations in Be main chamber tiles made by extrapolation of measurements made around several castellations is at  $\sim 1 \times 10^{22}$  atoms [18], or about 10% of the main chamber inventory, see TABLE I.

## 5. Conclusion

The results of post-mortem analyses after ILW-2 mostly confirm the data and interpretations formed after ILW-1, such as the main area of deposition is at the top of the inner divertor, and that D retention is about an order of magnitude lower than for comparable operations with a carbon wall; this already offers the hope for ITER that T accumulation will not reach statutory limits before the scheduled divertor refurbishments, when the main deposits would be automatically removed. The pattern of strike points for ILW-2 differed from ILW-1 in that there was a larger fraction of strike points in the divertor corners. This resulted in a larger flux of impurities to the divertor corners with more deposition and D-retention in the shadowed regions. However, the majority of the deposits in the divertor were still at the top of Tile 1 and on the HFGC tiles. Although no spalling of friable layers have yet been observed in JET, much thicker layers will accumulate in the ITER divertor, so there may well also be dust/flakes to be removed from the bottom of the vessel. Build up in selected areas of ITER may be exacerbated because the discharge shape is prescribed, and there will be no variation in strike point positions.

The Be main chamber wall has survived intact, apart from some melt damage on the Dump Plate tiles in the roof of the vessel. A concern is that this melting has extended outwards from the region of damage in ILW-1 as well as in amplitude, and may occur during confined plasmas, not just from disruptions. Deposition in the main chamber is restricted to the sides of limiters (and small amounts in castellation gaps), and is believed to occur mostly during the limiter phase, and these deposits are very adherent. Whilst these deposits contain some of the D inventory listed in Table 1, the majority of the main chamber D inventory is near the surface as a result of implantation into the very large exposed areas, and it appears from ILW-2 data that the inventory was reduced by finishing the campaign in H (Section 4.1). This is encouraging for DT operation in ITER in three ways: Firstly, limiter phases will form a very small proportion of the overall discharge periods (whereas in JET it may typically be 30%), secondly, the implantation depth is limited, so the amount of trapped T will not accumulate,

and thirdly, most of the T is accessible for removal by isotope exchange in clean-up operations with H or D fuelling.

Analysis of the bulk W Tile 5 from ILW-1 has been completed; overall these tiles account for only a small percentage of the global accountancy for ILW-1, as shown in TABLE I, demonstrating that in ITER implantation of H isotopes into the large areas of solid W will not be significant.

This work has been carried out within the framework of the EUROfusion Consortium and has received funding from the Euratom research and training programme 2014-2018 under grant agreement No 633053. The views and opinions expressed herein do not necessarily reflect those of the European Commission

## 6. References

- [1] KEILHACKER, M., WATKINS, M.L., JET TEAM, D-T experiments in the JET tokamak, *J. Nucl. Mater.* **266-269** (1999) 1.
- [2] ANDREW, P. et al., The tritium cleanup experiment in JET, *J. Nucl. Mater.* **196-198** (1992) 143.
- [3] MATTHEWS, G.F. et al., JET ITER-like wall—overview and experimental programme, *Phys. Scr.* **T145** (2011) 014001.
- [4] BREZINSEK, S. et al., Fuel retention studies with the ITER-Like Wall in JET, *Nucl. Fusion* **53** 8 (2013) 083023.
- [5] LOARER, T. et al., Comparison of long term fuel retention in JET between carbon and the ITER-Like Wall, *J. Nucl. Mater.* **438** (2013) S108.
- [6] HEINOLA, K. et al., Long-term fuel retention in JET ITER-like wall, *Phys. Scr.* **T167** (2016) 014075.
- [7] COAD, J.P. et al., Overview of JET post-mortem results following the 2007–9 operational period, and comparisons with previous campaigns, *Phys. Scr.* **T145** (2011) 014003.
- [8] COAD, J.P. et al., Diagnostics for studying deposition and erosion processes in JET, *Fusion Eng. Des.* **74** 1-4 (2005) 745.
- [9] WIDDOWSON, A. et al., Comparison of JET main chamber erosion with dust collected in the divertor, *J. Nucl. Mater.* **438** (2013) S827.
- [10] BARON-WIECHEC, A. et al., First dust study in JET with the ITER-like wall: sampling, analysis and classification, *Nucl. Fusion* **55** 11 (2015) 113033.
- [11] FORTUNE-ZALESNA, E. et al., Studies of Dust from JET with the ITER-Like Wall: Composition and Internal Structure, *Submitt. to Nucl. Mater. Eng.* (2016).
- [12] BARON-WIECHEC, A. et al., Global erosion and deposition patterns in JET with the ITER-like wall, *J. Nucl. Mater.* **463** (2015) 157.
- [13] MAYER, M. et al., Erosion and deposition in the JET divertor during the first ILW campaign, *Phys. Scr.* **T167** (2016) 014051.
- [14] MAYER, M. et al., Erosion, Deposition and Deuterium Inventory of the Bulk Tungsten Divertor Tile during the First JET ITER-like Wall Campaign, 22nd International Conference on Plasma Surface Interactions in Controlled Fusion Devices, (2016).
- [15] MATTHEWS, G.F. et al., Melt damage to the JET ITER-like Wall and divertor, *Phys. Scr.* **T167** (2016) 014070.
- [16] WIDDOWSON, A. et al., Material migration patterns and overview of first surface analysis of the JET ITER-like wall, *Phys. Scr.* **T159** (2014) 014010.
- [17] MAYER, M. et al., Erosion at the inner wall of JET during the discharge campaigns 2001–2009, *J. Nucl. Mater.* **438** (2013) S780.
- [18] RUBEL, M. et al., The role and application of ion beam analysis for studies of plasma-facing components in controlled fusion devices, **371** (2016) 4.